Title
Design of a Structure for Assembly and Cooling the Magnet of the Next-Generation 45 GHz ECR Ion Source MARS-D

Journal
IEEE Transactions on Applied Superconductivity, 36(3)

ISSN
1051-8223

Authors
Xu, Lianrong
Benitez, Janilee
Duran, Jaime Cruz
et al.

Publication Date
2026

DOI
10.1109/tasc.2025.3641911

Design of a Structure for Assembly and Cooling the Magnet of the Next-generation 45 GHz ECR Ion Source MARS-D

Lianrong Xu, Janilee Benitez, Jaime Cruz Duran, Paolo Ferracin, Member, IEEE, Mariusz Juchno, Larry Phair, Damon Todd, Li Wang, Ye Yang

[1] ***Abstract*—The current Electron Cyclotron Resonance Ion Sources (ECRISs), constructed with Nb-Ti wires and the conventional racetrack-and-solenoid structure, have achieved operating frequencies up to 28 GHz and utilized about 90% of the critical current of the Nb-Ti wire. A Mixed Axial and Radial field System Demonstrator (MARS-D) is being developed at Lawrence Berkeley National Laboratory (LBNL). This system, which consists of an innovative hexagonal Closed-Loop Coil (CLC) and a set of solenoids, can generate higher magnetic fields (up to 150%) while requiring only about 50% of the superconducting wire, enabling Nb-Ti wires to be used in the next-generation 45 GHz ECRIS. However, the assembly and cooling of such an efficient and compact magnet are particularly challenging due to the small radial gap between the CLC and solenoids, as well as the tight operating temperature margin. To address these challenges, a structure was developed that combines a three-section radially split solenoid mandrel with a series of shrink-fit reinforcement rings and cooling channels. This paper presents the detailed structure, manufacturing method, assembly procedure, impregnation method, mechanical Finite Element Analysis (FEA) comparison, and thermal FEA comparison.**

***Index Terms* — ECR ion sources, magnet structure, superconducting magnets.**

I. INTRODUCTION

The current Electron Cyclotron Resonance Ion Sources (ECRISs) use Nb-Ti wires and a conventional racetrack-and-solenoid structure to achieve an axial magnetic field of 4.0 T and a radial field of 2.0 T, supporting an operating frequency up to 28 GHz and utilizing approximately 90% of the critical current of the Nb-Ti wire [1-7]. The next generation of ECRISs will be designed to operate at significantly higher magnetic fields and frequencies, meeting the demanding ion-beam-intensity requirements for future heavy-ion accelerators and upgrades to existing facilities. Using Nb_3Sn wires is an option to achieve higher magnetic fields. However, Nb_3Sn wires introduce several challenges due to strong interaction forces that affect the critical current of Nb_3Sn, the brittleness of the wire, and the complex reaction process involved in fabrication [8-11]. A novel Mixed Axial and Radial field System (MARS) consisting of a hexagonal Closed-Loop Coil (CLC) and a set of solenoids combined with a hexagonal plasma chamber is highly effective at generating the required higher magnetic fields. 1. The primary advantage of MARS is its ability to produce higher magnetic fields (up to 1.5 times) than the conventional magnet structure within the material limitations of the superconducting wire being used, while requiring only about half the amount of superconducting wire. This significant advantage makes MARS a promising magnet design for future ECRISs. To demonstrate the suitability of the MARS magnet for use in ECRISs, a system named MARS-D, featuring a Nb-Ti MARS magnet, is currently under development at Lawrence Berkeley National Laboratory (LBNL). The optimized design of this magnet is expected to achieve magnetic field strengths of 5.7 T axially and 3.0 T radially, supporting operation at frequencies up to 45 GHz [12-14]. However, the fabrication of the hexagonal CLC is highly challenging due to its complex winding geometry, which was discussed in the previous paper [15]. Likewise, the assembly and cooling of such an efficient and compact magnet are particularly challenging due to the small radial gap (5 mm) between the CLC and solenoids, and the tight operating temperature margin (0.6 K). To overcome these challenges, a structure was developed that combines a three-section radially split solenoid mandrel with a series of shrink-fit reinforcement rings and cooling channels. Mechanical Finite Element Analysis (FEA) results demonstrated that the maximum stress in the three-section solenoid mandrel and the coils were similar to those of a single solenoid mandrel. Thermal FEA also indicated that the cooling channels significantly improved cooling efficiency compared to a solid solenoid mandrel. Six temperature sensors were installed near the hot spots in the CLC to monitor cooling temperatures and verify cooling performance.

II. COLD MASS STRUCTURES

The MARS magnet assembly is encapsulated by cold irons and applied preloads, as shown in Fig. 1 and Fig. 2. The cold irons shield and improve the magnetic field, preventing the eddy currents in the thermal shield and avoiding the influence of the axial magnetic force on the cold mass suspensions. The cold irons also increase the heat capacity of the cold mass, slowing

1This work was supported by the U.S. Department of Energy, Office of Science, Office of High Energy and Nuclear Physics under contract number DE-FOA-0002670. *(Corresponding author: Lianrong Xu).*

Lianrong Xu, J. Benitez, J. Cruz Duran, P. Ferracin, M. Juchno, L. Phair, D. Todd, L. Wang, Y. Yang are with the Lawrence Berkeley National Laboratory, Berkeley, CA 94720 USA (e-mail: lrxu@ lbl.gov).

Grammar in this manuscript was corrected with the assistance of Grammerly.

Color versions of one or more of the figures in this article are available online at http://ieeexplore.ieee.org down the temperature rise after quench. The aluminum clamping rods and nuts clamp both end plates to apply axial preload. The bladders and keys are inserted into the iron yokes between the magnet assembly and the aluminum clamping cylinder to apply radial preload [16]. The iron yokes are shorter than the solenoid mandrels and clamping cylinder to compensate for cooling shrinkage and to leave a space for liquid helium to pass through.

The iron yokes are divided into six sets along the clamping rods, leaving spaces for liquid helium to pass through. At the same angles, six axial channels and thirty (5x6) radial channels pass through the solenoid mandrels, twelve (2x6) radial channels pass through the clamping cylinder, eighteen axial channels and twelve radial channels pass through both end plates. All these internal liquid helium channels are interconnected, ensuring there are no blind cavities that could trap helium bubbles. This structure allows liquid helium to be brought as close as possible to the magnet, thereby effectively cooling the magnet.

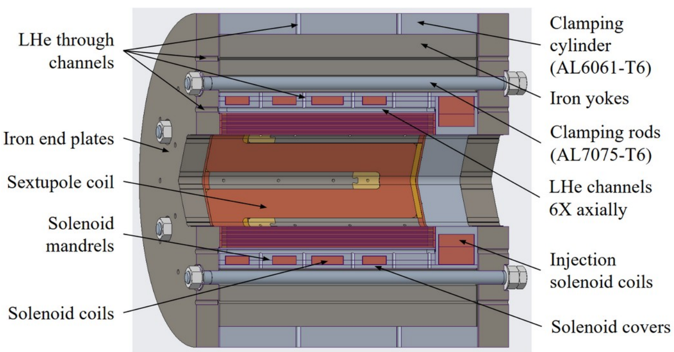

Fig. 1. Cold mass structures (a)

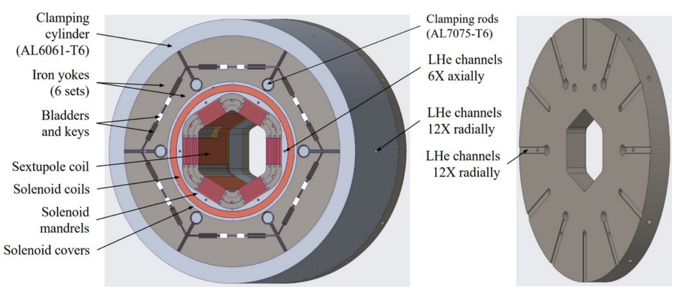

Fig. 2. Cold mass structures (b)

Ⅲ. SOLENOID MANDREL STRUCTURES

A. Conventional Single Mandrel

As shown in Fig. 3, a conventional single mandrel is simpler and easier to fabricate. However, the radial gap between the CLC and solenoids is only 5 mm. Sliding the CLC into the solenoid mandrel requires at least 1.5 mm of gap, resulting in a wall thickness of only 3.5 mm, which will cause large deformation. Furthermore, filling the 1.5 mm gap is challenging. Using pure epoxy for filling is not a wise choice due to its low strength and poor thermal conductivity.

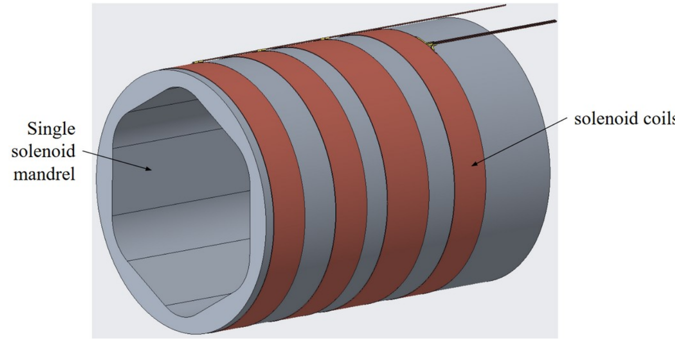

Fig. 3. Conventional single mandrel structure

B. Three-section Mandrel

To overcome the assembly challenges, a three-section mandrel structure was developed, as shown in Fig. 4. The solenoid mandrel is divided into three sections, which are aligned and assembled using pins and shrink-fit reinforcement rings. Six axial liquid helium channels and thirty radial liquid helium channels are employed to enhance cooling efficiency.

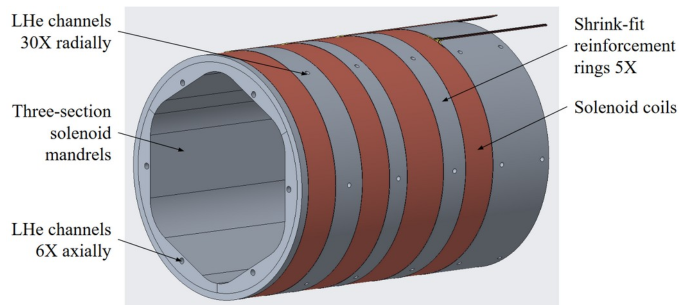

Fig. 4. Three-section mandrel structure

Ⅳ. THREE-SECTION MANDREL MANUFACTURING

The fabrication of the three-section mandrel requires a specialized manufacturing process, as shown in Fig. 5. Initially, three identical cylindrical sectors are produced separately. These sectors are then assembled into a complete cylinder using dowel pins for precise alignment, and the assembled cylinder is secured with hose clamps. The assembled cylinder serves as a semi-finished component for subsequent machining operations.

During the final manufacturing stage, the assembly is firmly held in place using hose clamps or equivalent fixtures to ensure dimensional stability. The outer diameter, overall length, and groove geometry are precisely machined on a lathe. Accurate control of the outer diameter is essential, as it interfaces with reinforcement rings through a shrink-fit connection. The internal hexagonal features are subsequently fabricated using wire Electrical Discharge Machining (EDM), ensuring high geometric precision. Finally, the sidewall notches are produced via Computer Numerical Control (CNC) machining.

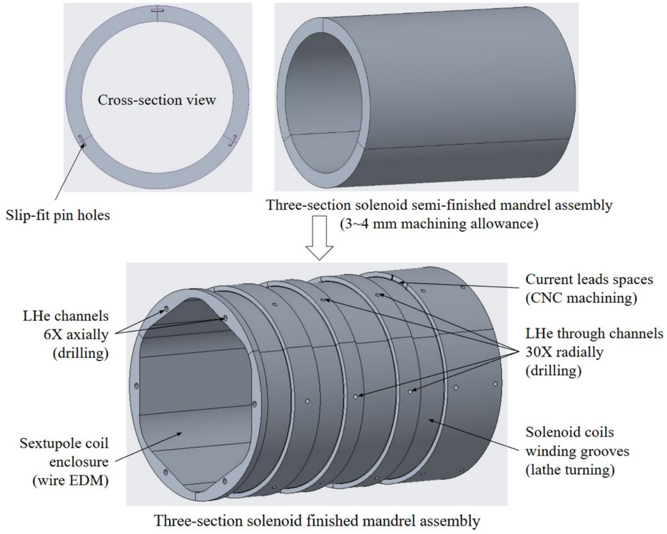

Fig. 5. Three-section mandrel manufacturing

V. THREE-SECTION MANDREL ASSEMBLY

The assembly of the three-section mandrel requires a specialized procedure, as shown in Fig. 6. Once assembled, the three-section mandrel will not be disassembled throughout the entire process to maintain geometric stability and alignment. Six turnbuckles are employed to regulate the opening and closing of the mandrel assembly. A uniform opening of 10 mm provides a 6 mm clearance, facilitating easy insertion of the CLC.

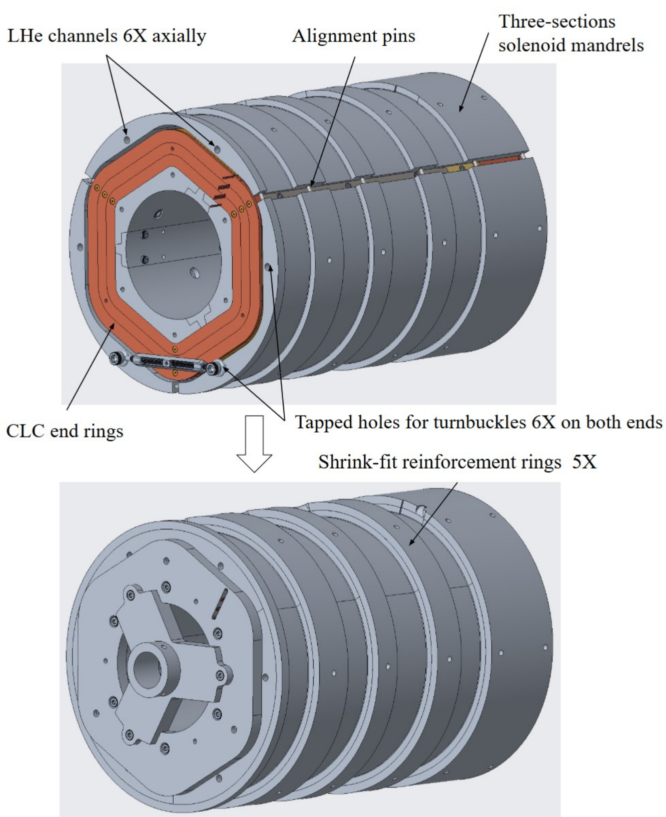

Fig. 6. Three-section mandrel assembly

After positioning the CLC, the three-section mandrel will be closed slowly and evenly, and secured using hose clamps positioned along the winding grooves, ensuring precise alignment with the hexagonal end rings of the CLC. Subsequently, the reinforcement rings are heated to 185 °C, causing their inner diameters to expand from 381 mm to 382.5 mm to create the necessary clearance for installation. Once the shrink-fit reinforcement rings are installed and cooled, the hose clamps are removed, and the mandrel assembly is prepared for subsequent solenoid coil winding.

VI. MAGNET IMPREGNATION

After the solenoid coils are wound onto the mandrel assembly, the CLC and solenoid coils will be impregnated together with CTD-101K epoxy in a vertical vacuum chamber and cured at 135°C. Six solenoid covers are used as epoxy enclosures. All the seams and holes are sealed with Room Temperature Vulcanizing (RTV) silicone and O-ring rods. A mold release agent is applied to surfaces that will contact the epoxy to facilitate demolding. The epoxy flow routes are shown in Fig. 7.

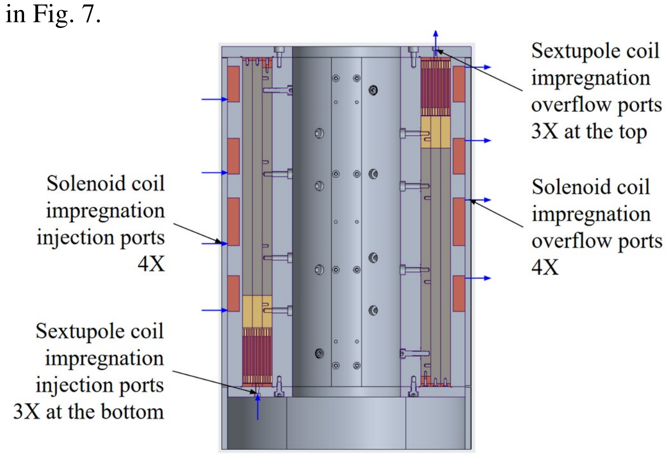

Fig. 7. Magnet impregnation

VII. MECHANICAL FEA COMPARISON

Mechanical Finite Element Analysis (FEA) of a single solenoid mandrel and coils was performed and discussed in a previous paper [16]. Later, the FEA was re-performed using a three-section solenoid mandrel. The results demonstrated that the stresses and contact pressures of the three-section solenoid mandrel and coils were comparable to those of a single solenoid mandrel. Fig. 8 shows some of the results.

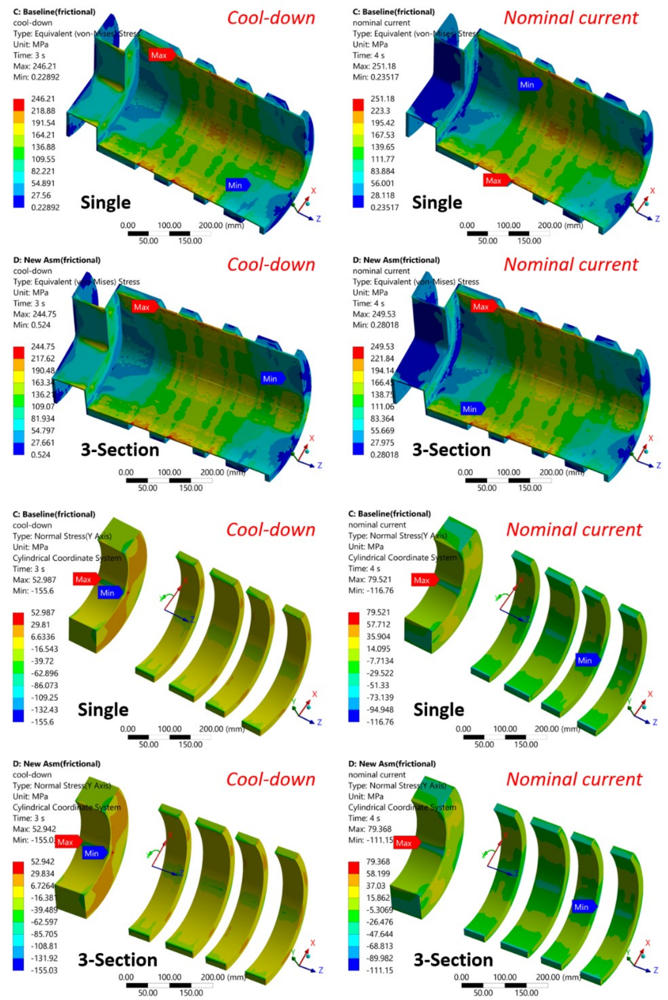

Fig. 8. Stress FEA and comparison

Ⅷ. THERMAL FEA COMPARISON

The entire cold mass is bath-cooled in liquid helium to ensure stable superconducting operation. The cooling efficiency of the cryogenic system is critical because of the narrow operating temperature margin. Electromagnetic design calculations and analyses indicate that the operating temperature margin is approximately 0.6 K, with quenching likely to occur if the temperature exceeds 4.8 K. During regular operation, dynamic heat loads from the ECR plasma are applied to the magnet. Additionally, during current ramping or deramping, hysteresis losses introduce an estimated heat load of approximately 1.1 W, which can elevate the coil temperature and potentially trigger a quench. The magnitude of hysteresis loss is directly correlated with the current ramp rate. Cryogenic calculations revealed that, following a quench, the temperature of the cold mass can rise to approximately 90 K and must be cooled back to 4.2 K. Enhancing cooling efficiency not only mitigates the risk of quenching but also reduces the time and liquid helium consumption required for magnet training and testing.

Transient thermal FEA indicated that the internal liquid helium channels significantly improved the cooling efficiency, as shown in Fig. 9.

Case A: Only the exposed surfaces of the cold mass were in contact with liquid helium.

Case B: In addition to the exposed surfaces of the cold mass that were in contact with liquid helium, liquid helium also passed through the internal liquid helium channels.

From the same initial temperature to 4.2 K, the cooling time of case B is about 40% of that of case A. In other words, the cooling efficiency of case B is approximately 2.5 times that of case A, regardless of the initial temperature.

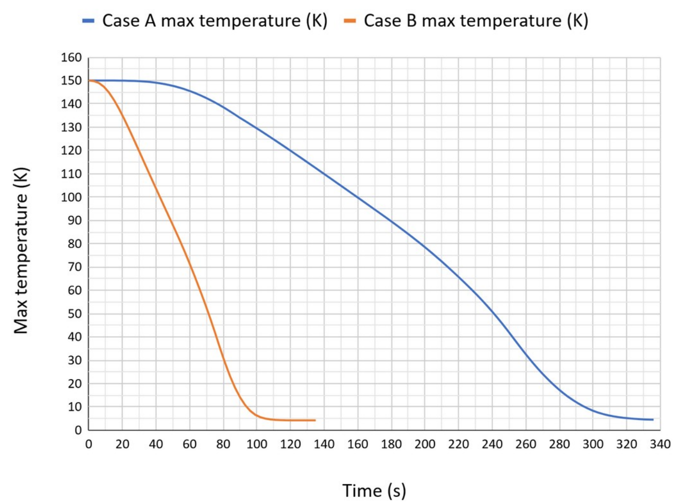

Fig. 9. Dynamic cooling FEA and comparison

Ⅸ. CONCLUSION

The three-section mandrel structure simplifies assembly, alignment, clamping, and impregnation processes, saving time and cost. It also improves mechanical strength and thermal conduction as there is no gap between the CLC and the solenoid mandrel. The internal liquid helium channels significantly improve the cooling efficiency.

REFERENCES

[1] C. M. Lyneis, Z. Q. Xie, and C. E. Taylor, "Development of the third generation electron cyclotron resonance ion source," *Review of Scientific Instruments*, vol. 69, no. 2, pp. 682, Feb. 1998, doi: 10.1063/1.1149169.

[2] S. Gammino, G. Ciavola, L. Celona, D. Hitz, A. Girard, and G. Melin, "Operation of the SERSE superconducting electron cyclotron resonance ion source at 28 GHz," *Review of Scientific Instruments*, vol. 72, no. 11, pp. 4090, Nov. 2001, doi: 10.1063/1.1405786.

[3] T. Nakagawa *et al.*, "Effect of magnetic-field configuration on the beam intensity from electron cyclotron resonance ion source and RIKEN superconducting electron cyclotron resonance ion source," *Review of Scientific Instruments*, vol. 77, no. 3, pp. A304, Mar. 2006, doi: 10.1063/1.2149304.

[4] H. W. Zhao *et al.*, "Advanced superconducting electron cyclotron resonance ion source SECRAL: Design, construction, and the first test result," *Review of Scientific Instruments*, vol. 77, no. 3, pp. A333, Mar. 2006, doi: 10.1063/1.2149307.

[5] P. A. Zavodszky *et al.*, "Status report on the design and construction of the Superconducting Source for Ions at the National Superconducting Cyclotron Laboratory/Michigan State University," *Review of Scientific Instruments*, vol. 77, no. 3, pp. A334, Mar. 2006, doi: 10.1063/1.2162855.

[6] G. Ciavola *et al.*, "A status report of the multipurpose superconducting electron cyclotron resonance ion source," *Review of Scientific Instruments*, vol. 79, no. 2, pp. A326, Feb. 2008, doi: 10.1063/1.2812336.

[7] H. Felice *et al*., "Design of a superconducting 28 GHz ion source magnet for FRIB using a shell-based support structure," *IEEE Trans. Appl. Supercond.*, vol. 25, no. 3, Jun. 2015, doi: 10.1109/TASC.2014.2377730.

[8] C. M. Lyneis *et al.*, "Fourth generation electron cyclotron resonance ion sources (invited)," *Review of Scientific Instruments*, vol. 79, no. 2, pp. A321, Feb. 2008, doi: 10.1063/1.2816793.

[9] S. Prestemon *et al*., "Design of a Nb_3Sn magnet for a 4th generation ECR ion source," *IEEE Trans. Appl. Supercond.*, vol. 19, no. 3, pp. 1336, Jun. 2009, doi: 10.1109/TASC.2009.2017719.

[10] L. Sun *et al*., "Progress on the development of key technologies for the fourth generation ECR ion source FECR," *Journal of Physics: Conference Series*, vol. 2244, no. 1, pp. 012021, Apr. 2022, doi: 10.1088/1742-6596/2244/1/012021.

[11] T. Shen *et al*., "Design and Development of a 28 GHz Nb3Sn ECR Ion Source Superconducting Magnet," *IEEE Trans. Appl. Supercond.*, vol. 34, no. 5, Aug. 2024, doi: 10.1109/TASC.2024.3358767.

[12] D. Z. Xie, "A new structure of superconducting magnetic system for 50 GHz operations," *Review of Scientific Instruments*, vol. 83, no. 2, pp. A302, Feb. 2012, doi: 10.1063/1.3655530.

[13] D. Z. Xie *et al*., "Design of a new superconducting magnet system for high strength minimum-B fields for ECRIS," *IEEE Trans. Appl. Supercond.*, vol. 26, no. 4, Jun. 2016, doi: 10.1109/TASC.2015.2511928.

[14] D. Z. Xie *et al*., "Development status of a next generation ECRIS: MARS-D at LBNL," *Review of Scientific Instruments*, vol. 87, no. 2, pp. A702, Sep. 2016, doi: 10.1063/1.4931713.

[15] L. Xu *et al*., "Fabrication of a Nb-Ti Superconducting Closed-Loop Coil for the Next-Generation 45 GHz ECR Ion Source MARS-D," *IEEE Trans. Appl. Supercond.*, vol. 35, no. 5, Aug. 2025, doi: 10.1109/TASC.2025.3542743.

[16] M. Juchno *et al*., "Shell-Based Support Structure for the 45 GHz ECR Ion Source MARS-D," *IEEE Trans. Appl. Supercond.*, vol. 32, no. 6, Sep. 2022, doi: 10.1109/TASC.2022.3158375.